Published in final edited form as:
Cell Rep. 2012 December 27; 2(6): 1762–1773. doi:10.1016/j.celrep.2012.10.026.

Tracing Conidial Fate and Measuring Host Cell Antifungal Activity Using a Reporter of Microbial Viability in the Lung

Anupam Jhingran[1], **Katrina B. Mar**[1], **Debra K. Kumasaka**[1], **Sue E. Knoblaugh**[2], **Lisa Y. Ngo**[1], **Brahm H. Segal**[3], **Yoichiro Iwakura**[4], **Clifford A. Lowell**[5], **Jessica A. Hamerman**[6], **Xin Lin**[7], and **Tobias M. Hohl**[1,*]

[1]Vaccine and Infectious Diseases Division

[2]Comparative Medicine Shared Resources Fred Hutchinson Cancer Research Center, Seattle, WA 98109, USA

[3]Department of Immunology, Roswell Park Cancer Institute, Buffalo, NY 14263, USA

[4]Research Institute for Biomedical Sciences, Tokyo University of Science, Noda, Chiba 278-0022, Japan

[5]Immunology Program and the Department of Laboratory Medicine, University of California at San Francisco, San Francisco, CA 94143, USA

[6]Immunology Program, Benaroya Research Institute, Seattle, WA 98101, USA

[7]Department of Molecular and Cellular Oncology, University of Texas, MD Anderson Cancer Center, Houston, TX 77030, USA

Abstract

Fluorescence can be harnessed to monitor microbial fate and to investigate functional outcomes of individual microbial cell-host cell encounters at portals of entry in native tissue environments. We illustrate this concept by introducing fluorescent *Aspergillus* reporter (FLARE) conidia that simultaneously report phagocytic uptake and fungal viability during cellular interactions with the murine respiratory innate immune system. Our studies using FLARE conidia reveal stepwise and cell-type-specific requirements for CARD9 and Syk, transducers of C-type lectin receptor and integrin signals, in neutrophil recruitment, conidial uptake, and conidial killing in the lung. By achieving single-event resolution in defined leukocyte populations, the FLARE method enables host cell profiling on the basis of pathogen uptake and killing and may be extended to other pathogens in diverse model host organisms to query molecular, cellular, and pharmacologic mechanisms that shape host-microbe interactions.

INTRODUCTION

The sequestration and killing of pathogenic microbes at portals of entry are fundamental properties of the immune system. Despite the importance of these processes, studies in microbial pathogenesis lack robust methods to quantify microbial uptake and killing by leukocytes in native tissue environments with single-encounter resolution. Studies with purified immune cells do not model the complexity and context of intact tissues, whereas in

*Correspondence: thohl@fhcrc.org.

SUPPLEMENTAL INFORMATION Supplemental information includes five figures and Extended Experimental Procedures and can be found with this article online at http://dx.doi.org/10. 1016/j.celrep.2012.10.026.

vivo studies of host-pathogen encounters often rely on surrogate endpoints, e.g., microbial tissue burden or host survival, that measure aggregate processes rather than individual cellular encounters.

Fluorescent proteins have long served as sensors of cellular environments, exemplified by genetically encodable probes that sense changes in ambient pH (Miesenböck et al., 1998). In pathogenesis studies, researchers have harnessed microbial fluorescent protein expression to report microbial localization, tissue burden, and host cell associations (Coombes and Robey, 2010). To measure host microbicidal activity with single-cell resolution, quantitation of both live and killed microbial cells represents a formidable obstacle, particularly for fluorescent microbes that are rapidly inactivated to nonfluorescent and, for many experimental purposes, invisible particles. Engineering microbes to emit a fluorescent signal coupled to loss of viability provides a potential solution to this obstacle.

Humans inhale mold conidia (asexual spores) daily. These infectious propagules do not divide into discrete cellular units but rather form tissue-invasive filaments when their growth is not checked by the respiratory innate immune system. The action of neutrophils and alveolar macrophages (AMs) prevents this transition, with most infections resolving in an asymptomatic fashion. However, defects in neutrophil trafficking (Bonnett et al., 2006; Mehrad et al., 1999), number (Gerson et al., 1984;Mircescu et al., 2009), or function (Park and Mehrad, 2009) predispose to invasive disease, commonly caused by *Aspergillus fumigatus*. Although the oxidative burst, degranulation, nutrient sequestration, and antimicrobial peptides contribute to neutrophil antifungal activity (Brown, 2011), understanding the mechanisms that control neutrophil conidiacidal activity in vivo has been difficult to achieve.

Neutrophil activation by *A. fumigatus* conidia is attributed to stage-specific exposure of C-type lectin receptor (CLR) and Toll-like receptor (TLR) ligands. The CLR Dectin-1 binds β-(1,3)-glucan on germinating conidia (Gersuk et al., 2006; Hohl et al., 2005; Steele et al., 2005) and transduces signals via an intracellular immunoreceptor tyrosine-based activation motif (ITAM)-like domain to spleen tyrosine kinase (Syk) and to caspase recruitment domain adaptor protein 9 (CARD9) (Mócsai et al., 2010). Syk- and CARD9-mediated antifungal immunity is principally ascribed to defects in cytokine regulation by macrophages and dendritic cells (DCs) (Gross et al., 2006; Hara et al., 2007; Hsu et al., 2007), resulting in defects in the formation of T helper 17 (Th17) cells (LeibundGut-Landmann et al., 2007) and in susceptibility to mucosal candidiasis in humans (Glocker et al., 2009). Other studies link Dectin-1 (Li et al., 2011; Werner et al., 2009), CARD9 (Wu et al., 2009), integrins, and Syk to the activation of antimicrobial effectors, the latter exemplified by b2-integrin (CD18) and Syk-dependent neutrophil NADPH oxidase activity against sterile fungal hyphae (Boyle et al., 2011; Leal et al., 2012). In vitro, $Syk^{(-/-)}$ neutrophils are defective in the uptake of opsonized bacteria and in degranulation, resulting in delayed staphylococcal clearance (Van Ziffle and Lowell, 2009). Thus, despite increasing evidence that links CARD9 and Syk to cytokine regulation and to antimicrobial effector functions, the role and timing of CARD9 and Syk in neutrophil defense against inhaled mold conidia remain poorly defined.

Although fluorescent *A. fumigatus* strains have been generated for in vitro and in vivo applications (Balajee and Marr, 2002; Hohl et al., 2009; Leal et al., 2010; Wasylnka and Moore, 2002), tracing the outcome of fungal-host cell interactions remains elusive. In this study, we harness fluorescence to trace the outcome of conidia-host cell interactions in murine lungs. Herein, we introduce a *fl*uorescent *Aspergillus re*porter (FLARE) strain that emits two fluorescent signals—one to report conidial viability, the second to trace conidia independent of viability—to visualize and quantify conidial uptake and killing and to resolve sequential steps of neutrophil function during respiratory *A. fumigatus* challenge.

Monitoring conidial fate with the FLARE method demonstrates that CARD9 is essential for lung neutrophil recruitment and for optimal phagocytic and conidiacidal responses, whereas Syk is indispensable for conidial uptake and killing. These studies indicate sequential and cell-type-specific roles for CARD9 and Syk in neutrophil-mediated clearance of inhaled mold spores. Our results illustrate the utility of a microbial reporter of viability to facilitate functional analysis of microbial cell-host cell encounters in native tissue environments.

RESULTS

A Fluorescent Reporter Distinguishes Live and Killed Conidia

The FLARE strain was developed to trace conidial fate and enable functional analysis of leukocyte conidiacidal activity in the lung. We reasoned that conidial expression of a red fluorescent protein variant, dsRed, could act as a viability indicator because dsRed has an ~45 min half-life in phagolysosomes (Maselli et al., 2002), the compartment implicated in conidial killing (Ibrahim-Granet et al., 2003). Given that killed conidia form crescent-shaped ghosts within phagocytes (Philippe et al., 2003), we attached a fluorescent tracer dye (Alexa Fluor 633; AF633) to the surface of live dsRed$^+$ conidia (Figure 1A) with the aim of detecting a signal from the tracer dye after conidial cell death. The modifications introduced into the *A. fumigatus* 293 parental strain did not alter bone marrow macrophage (BMM) cytokine responses to conidia (Figure 1B), suggesting that conidial dsRed expression and chemical labeling with AF633 do not interfere with or enhance macrophage responsiveness to conidia.

For measuring dsRed and AF633 fluorescence under conidiacidal conditions in vitro, dsRed$^+$AF633$^+$ conidia were exposed to increasing concentrations of H_2O_2, analyzed by flow cytometry, and plated for colony-forming units (cfu). dsRed$^+$AF633$^+$ conidia lost dsRed but retained AF633 fluorescence at conidiacidal H_2O_2 concentrations (Figure 1C). Extinction of dsRed fluorescence and the shift to a single fluorescent emission correlated with conidial killing, as measured by cfu analysis. Similar results were obtained when dsRed$^+$AF633$^+$ conidia were treated with 30 μM HOCl (data not shown). dsRed$^+$AF633$^+$ conidia are referred to as FLARE conidia hereafter.

FLARE Conidia Report Conidial Fate In Vivo

To assess dsRed as a reporter of conidial viability in vivo, C57BL/6 mice were infected with 3×10^7 FLARE conidia via the intratracheal (i.t.) route, and single-cell lung suspensions were analyzed for dsRed and AF633 fluorescence (Figure 1D). For CD45$^+$ CD11b$^+$Ly6G$^+$ lung neutrophils, flow cytometric analysis gave rise to dsRed$^-$AF633$^-$ (Figure 1E, tan gate), dsRed$^-$AF633$^+$ (Figure 1E, blue gate), and dsRed$^+$AF633$^+$ (Figure 1E, red gate) cell populations. Similar results were observed for lung monocytes, macrophages, and CD11b$^+$ DCs (data not shown). Control mice infected with singly labeled conidia (AF633 or dsRed) gave rise to expected fluorophore-positive and fluorophore-negative neutrophil populations (Figures 1F and 1G).

To determine whether dsRed$^+$AF633$^+$ leukocytes contain live conidia, dsRed$^+$AF633$^+$ lung neutrophils, macrophages, and CD11b$^+$ DCs were sorted and plated for cfu. dsRed$^+$AF633$^+$ lung leukocytes harbored live conidia because these cells contain ~0.5–0.75 cfu per sorted event (Figure 1H, red bars). Dually fluorescent conidia were visible in dsRed$^+$AF633$^+$ neutrophils by fluorescence microscopy (Figure 1I) or imaging cytometry (Figure 1L). In contrast, dsRed$^-$AF633$^+$ lung leukocytes harbored killed conidia by cfu analysis, with <0.005 cfu per sorted event (Figure 1H, blue bars), despite clear visualization of AF633$^+$ conidia in neutrophils (Figures 1J and 1M). dsRed$^-$AF633$^-$ neutrophils (Figure 1E, tan gate) did not contain conidia by imaging cytometry (Figure 1K) and thus represent bystander

cells. In sum, these data indicate that FLARE-dependent signals can distinguish bystander and fungus-engaged leukocytes and report the viability status of engulfed conidia.

To examine whether conidial killing is associated with leukocyte uptake, the frequency of live and killed conidia was compared in $CD45^-$ and in $CD45^+$ lung cell populations. Conidial viability was 72% at 12 hr postinfection (p.i.) and 61% at 36 hr p.i. in the $CD45^-$ gate (Figures 2A and 2B). The corresponding values were 18% and 7% in the $CD45^+$ gate (Figures 2A and 2B), indicating that leukocyte uptake generally precedes conidial killing. Neutrophils represent the predominant leukocyte subset that engulfs and kills FLARE conidia in infected lungs (Figures 2C–2E).

FLARE Conidia Detect Defects in Neutrophil Conidiacidal Activity

The molecular defect in chronic granulomatous disease (CGD) results in NADPH oxidase deficiency and is associated with an ~40% lifetime risk of invasive aspergillosis (IA). To validate the FLARE strain, we generated and infected mice that harbor congenically marked NADPH oxidase-sufficient ($p47^{phox(+/+)}$) and -deficient ($p47^{phox(-/-)}$) neutrophils. For all ensuing experiments, neutrophil conidial uptake refers to the frequency of fungus-engaged ($dsRed^+AF633^+$ and $dsRed^-AF633^+$) neutrophils, whereas neutrophil conidial viability refers to the frequency of neutrophils that contain live conidia ($dsRed^+AF633^+$ neutrophils) among all fungus-engaged neutrophils. As expected, conidial uptake was indistinguishable among $p47^{phox(+/+)}$ and $p47^{phox(-/-)}$ neutrophils (Figures 3A and 3B). Conidial viability was higher in $p47^{phox(-/-)}$ than in $p47^{phox(+/+)}$ neutrophils at 12 hr (19.2% ± 1.2% versus 7.1% ± 2.3%) and 36 hr (28.8% ± 2.9% versus 14.7% ± 1.1%) p.i. (Figure 3C). Although conidial killing was superior in $p47^{phox(+/+)}$ neutrophils in all experiments and at all time points examined, the majority of conidia were killed in $p47^{phox(-/-)}$ neutrophils, consistent with a partial NADPH oxidase dependency for neutrophil conidiacidal activity.

Application of FLARE Conidia to Map CARD9-Dependent Neutrophil Antifungal Activity

The adaptor protein CARD9 integrates signals from Syk-coupled CLRs, e.g., Dectin-1, Dectin-2, and Mincle, implicated in fungal cell wall recognition (LeibundGut-Landmann et al., 2012), though Syk may not be required for all CLR-induced functions (Herre et al., 2004; Underhill et al., 2005). In the ensuing experiments, we harnessed FLARE conidia to investigate the role of CARD9 and Syk in regulating neutrophil anticonidial activity in the lung.

CARD9 is essential for murine survival following i.t. challenge with 8×10^7 *A. fumigatus* conidia (Figure 4A). We observed 67% mortality for $CARD9^{(-/-)}$ mice at 30 days p.i. and no mortality in C57BL/6 and $Dectin\text{-}1^{(-/-)}$ mice. Lungs of $CARD9^{(-/-)}$ survivors analyzed 30 days p.i. contained multifocal pyogranulomatous lesions with numerous fungal hyphae arranged within the central core (Figures S1A and S1B). Lung hyphal lesions were absent in WT (C57BL/6) and $Dectin\text{-}1^{(-/-)}$ mice (data not shown).

To determine whether CARD9 regulates early lung inflammatory responses, cytokine levels and neutrophil influx were compared in $CARD9^{(-/-)}$, $Dectin\text{-}1^{(-/-)}$, and WT mice following conidial challenge. Respiratory fungal infection induced cytokine responses in all groups (Figure S2A), though lung CXCL1, CXCL2, TNF, IL-1β, and IL-17A levels were markedly reduced in $CARD9^{(-/-)}$ mice, but not in $Dectin\text{-}1^{(-/-)}$ mice, compared to WT mice at 36 hr p.i. (Figures 4B and S2A) despite similar fungal burdens at this time point (Figure S2B). Impaired lung CXCL1 and CXCL2 levels in $CARD9^{(-/-)}$ mice correlated with a reduced lung neutrophil influx at 36 hr and 72 hr p.i. (Figure 4C). Consistent with these observations, CARD9 was required for BMM and BM dendritic cell (BMDC) TNF and CXCL2 responses to all *A. fumigatus* morphotypes, with variable and cell-type-specific contributions of the

CARD9-coupled CLRs Dectin-1 and Dectin-2 (Figures S2C–S2H). These data support a model in which CARD9 regulates lung neutrophil influx through the production of neutrophil-recruiting cues.

To determine whether CARD9 controls neutrophil conidiacidal activity, lung neutrophil conidial uptake was measured in FLARE-infected mice and found to be lower in CARD9$^{(-/-)}$ mice than in WT mice at 12, 36, and 72 hr p.i. (Figures 4D and 4E). Similar results were seen in Dectin-1$^{(-/-)}$ mice at 12 hr p.i., but not at later time points (Figures 4D and 4E). To pool and compare data from multiple experiments, we normalized neutrophil conidial uptake and neutrophil conidial viability for each sample to the average value for WT neutrophils in the corresponding experiment. This analysis confirmed the conidial uptake defect in CARD9$^{(-/-)}$ mice (Figure 4F), a defect that cannot be attributed to defective neutrophil Dectin-1 expression (data not shown). An in vitro assay showed impaired conidial uptake by CARD9$^{(-/-)}$ and Dectin-1$^{(-/-)}$ BM neutrophils (Figures S3A and S3B), corroborating the in vivo results.

Conidia were more likely to be viable in lung neutrophils in CARD9$^{(-/-)}$ mice compared to WT or Dectin-1$^{(-/-)}$ mice at 36 and 72 hr p.i. (Figure 4G). On average, lung neutrophil conidial viability in CARD9$^{(-/-)}$ mice was 1.3-fold higher at 36 hr p.i. (10.7% ± 0.8% versus 8.2% ± 1.3%) and 3.1-fold higher at 72 hr p.i. (8.0% ± 0.7% versus 2.6% ± 0.3%) than in WT mice, indicating that neutrophils in CARD9$^{(-/-)}$ mice kill conidia less effectively than neutrophils in WT and Dectin-1$^{(-/-)}$ mice (Figure 4H). In vitro, CARD9 is dispensable for BM neutrophil ROS production following stimulation with swollen conidia (Figure 4I), suggesting that impaired NADPH oxidase activity is unlikely to account for the CARD9-dependent reduction in neutrophil conidiacidal activity. Conidial uptake and viability were not altered in AMs in CARD9$^{(-/-)}$ mice (Figures S4A–S4E), indicating cell-type-specific effects of CARD9 deficiency.

To relate CARD9-dependent defects in neutrophil function to a host defect in controlling conidial germination, mice were euthanized 72 hr p.i. and examined by histopathology. In silver-stained lung sections, germ tube formation was rare in WT and Dectin-1$^{(-/-)}$ mice (Figures 4J and 4K) and more common in CARD9$^{(-/-)}$ mice (Figure 4L, black arrows). Germlings accounted for 1%–2% of fungal elements in WT and Dectin-1$^{(-/-)}$ lungs and 4.5% of fungal elements in CARD9$^{(-/-)}$ lungs (Figure 4M). Consistent with the defect in controlling conidial germination, lung cfu were 7-fold higher in CARD9$^{(-/-)}$ mice than in Dectin-1$^{(-/-)}$ and WT mice at 6 days p.i. (Figure 4N). Thus, CARD9 controls neutrophil function during respiratory *A. fumigatus* infection, primarily by regulating lung neutrophil influx, and by mediating optimal neutrophil phagocytic and conidiacidal activity.

Application of FLARE Conidia to Map Syk-Dependent Neutrophil Antifungal Activity

Beyond acting as a transducer for CLRs, Syk is essential for neutrophil integrin (CD11b/CD18) signaling and has been linked to NADPH oxidase activity (Boyle et al., 2011; Mócsai et al., 2002). We examined the role of hematopoietic Syk and CD18 expression on neutrophil function using BM chimeric mice (Syk$^{(-/-)}$ → WT and CD18$^{(-/-)}$ → WT) because Syk deficiency causes an embryonic lethal phenotype (Mócsai et al., 2010). Syk$^{(-/-)}$ → WT mice appeared moribund 3–4 days p.i. with 2–5 × 10^7 conidia and succumbed rapidly, unlike Dectin-1$^{(-/-)}$ → WT or WT → WT mice (Figure 5A). The Syk mortality phenotype was not recapitulated in CD18$^{(-/-)}$ → WT mice (75% 18 day survival; WT → WT mice 100% 18 day survival, n = 8/group; p = 0.14). Lung neutrophil recruitment and lung cytokine responses were similar in Syk$^{(-/-)}$ → WT and WT → WT mice (Figures 5B and 5C). CD18$^{(-/-)}$ → WT mice did not exhibit a defect in lung neutrophil recruitment, with a trend toward higher lung neutrophil numbers than control mice (Figure S5A–S5D).

Syk$^{(-/-)}$→ WT mice develop IA rapidly because lung sections prepared 3 days p.i. revealed extensive, multifocal necrotic lesions admixed with masses of fungal hyphae (Figures 5D–5Fii). Widespread invasive hyphae were associated with intravascular thrombosis, hemorrhage, and obliteration of bronchoalveolar architecture (Figures 5D, 5Fi, and 5Fii). In contrast, control lung sections (WT → WT mice) did not contain hyphae and showed moderate inflammatory infiltrates (Figures 5G and 5H).

Because differences in neutrophil influx did not account for the development of IA in Syk$^{(-/-)}$ → WT mice, neutrophil function in Syk$^{(-/-)}$ → WT was examined with FLARE conidia. Syk$^{(-/-)}$ neutrophils were highly defective in conidial uptake in vivo at all time points examined (Figures 5I and 5J), a phenotype recapitulated in vitro with a >80% reduction in conidial uptake by Syk$^{(-/-)}$ BM neutrophils compared to WT neutrophils (Figure S3C). In contrast, Syk$^{(-/-)}$ AMs engulfed conidia as efficiently as WT AMs in the lung (Figures 5L and 5M). Syk$^{(-/-)}$ lung neutrophils had highly impaired conidiacidal activity because conidial viability was increased by 6.9-fold in Syk$^{(-/-)}$ lung (38.5% ± 12.8% versus 5.6% ± 0.8%) or by 2.5-fold in bronchoalveolar lavage (BAL) neutrophils (76.8% ± 12.8% versus 31.2% ± 5.3%) compared to WT counterparts (Figure 5K; data not shown). In contrast to CARD9$^{(-/-)}$ BM neutrophils, Syk$^{(-/-)}$ neutrophils failed to produce ROS when stimulated with swollen conidia in vitro (Figure 5O). Syk$^{(-/-)}$ AMs displayed impaired conidiacidal activity, indicating that Syk is required both for neutrophil and AM cytotoxic activity against conidia (Figure 5N). The Syk phenotype in neutrophil conidial uptake and viability was not recapitulated in vivo or in vitro in CD18$^{(-/-)}$ → WT mice or in CD18$^{(-/-)}$ BM neutrophils (Figures S5 and S3D). Thus, FLARE conidia reveal that Syk is essential for pulmonary *A. fumigatus* host defense by mediating neutrophil conidial uptake and killing. In aggregate, these results indicate that FLARE conidia report microbial viability in vivo and can distinguish cell-type-specific and sequential phenotypes associated with microbial cell uptake and killing by leukocytes in native tissue environments.

DISCUSSION

FLARE conidia attest to the principle that a fluorescent reporter of microbial viability can trace microbial fate and measure the outcome of microbial cell-host cell interactions in native tissue environments. Our studies indicate that FLARE conidia can measure phagocytic and cytotoxic properties of leukocytes with single-cell resolution, enabling parallel phenotypic analyses of distinct leukocyte subsets and of gene-deficient and gene-sufficient leukocytes within the same host. Measuring conidial fate using the FLARE principle is likely to facilitate leukocyte profiling on the basis of pathogen uptake and killing within physiologically relevant contexts. The method has the potential to be combined with imaging technology to explore temporal, anatomic, and cellular aspects of conidiacidal activity in the lung (Looney et al., 2011). FLARE conidia could be administered at other physiologically relevant portals of infections, e.g., nasal sinuses or corneal tissues (Leal et al., 2010; Rodriguez et al., 2007), to probe tissue- or organ-specific host defense mechanisms.

The approach described in this manuscript is likely to be applicable to other organisms and hosts. *A. fumigatus* belongs to a family of conidia-forming molds, many of which represent emerging pathogens in immune-compromised patients and in patients administered contaminated medical products, tragically illustrated in the 2012 United States fungal meningitis outbreak caused primarily by the dematiaceous mold, *Exserohilum rostratum* (Kauffman et al., 2012; Pettit et al., 2012). Similarly, the agents of mucormycosis, fusariosis, and scedosporiosis are transmitted by infectious conidia, typically by inhalation or cutaneous inoculation. Genetic manipulation of these organisms is likely to permit the generation of additional viability reporter strains for in vivo applications to study the

pathogenesis of and host immune responses to opportunistic molds (Mertens et al., 2006). Fluorescent fungal strains have recently been generated to monitor pathogenesis in intact transparent hosts (Brothers et al., 2011; Tobin et al., 2012), a favorable experimental setup to examine and harness reporters of microbial viability.

Different classes of organisms may require unique solutions to realize the principle of tracing microbial fate in a host. First, the large size of *A. fumigatus* conidia (~3 μm diameter) enables facile detection of single-cell encounters with leukocytes. Signal detection with smaller microbial cellular units, and within complex tissue environments, may impede measurements of microbial uptake and killing. Second, the tracer fluorophore in FLARE conidia is attached directly to resting conidia outside the host. For rapidly dividing microbial cells, dilution of the tracer fluorophore following cell division is likely to limit the number of generations during which microbial cell uptake and killing can be monitored. The technical solution presented in this manuscript, a hybrid combination of a genetically encodable viability reporter and a covalently linked tracer fluorophore, would be enhanced by incorporating a tracer fluorophore that is replenished during microbial growth and retains fluorescence ensuing microbial cell death. A tracer fluorophore with these properties may extend the temporal and spatial dimensions in which microbial cell-host cell interactions could be monitored.

Our studies with the FLARE strain indicate that conidial escape and lethal tissue invasion in CARD9$^{(-/-)}$ mice result from defective neutrophil influx and suboptimal neutrophil phagocytic and cytotoxic function. Syk controls neutrophil-dependent conidial uptake and mediates both neutrophil and AM cytotoxic activity, highlighting cell-type-specific function during fungal infection. These data demonstrate sequential and cell-type-specific requirements for CARD9 and Syk signaling during neutrophil-mediated conidial clearance in the lung. Different requirements for CARD9 and Syk in orchestrating neutrophil influx and activation are consistent with the observation that CARD9 can enhance TLR-driven cytokine responses to zymosan (Goodridge et al., 2009). A recent study identified Raf-1 as a downstream signaling component of Dectin-1 that contributes to NF-κB activation in a Syk-independent pathway (Gringhuis et al., 2009). Thus, phenotypic differences observed with CARD9 and hematopoietic Syk deficiency are consistent with the notion that these signal transducers integrate shared and unique afferent inputs and have distinct efferent outputs. Elucidating the relationship between these signaling molecules during complex microbial infections represents an active area of investigation.

The finding that *A. fumigatus* activates the CARD9-coupled receptors Dectin-1 and Dectin-2 extends prior studies on the role of Dectin-1 against *A. fumigatus* (Leal et al., 2010; Werner et al., 2009, 2011). In humans, one of two studies links a *Dectin-1* polymorphism (Y238X) to IA in allogeneic hematopoietic stem cell transplant (HCT) patients (Chai et al., 2011; Cunha et al., 2010). In mice, Dectin-1 deficiency is associated with enhanced mortality (Werner et al., 2009), whereas other studies report delayed or normal clearance (Cunha et al., 2010; Rivera et al., 2011). We did not observe a lung cytokine, fungal clearance, or mortality defect in Dectin-1$^{(-/-)}$ mice. However, our results do not imply that Dectin-1 is dispensable for murine host defense, given the role observed in neutrophil conidial uptake. Differences in the genetic background of the host (Carvalho et al., 2012), in fungal cell wall composition (Leal et al., 2010), and in experimental models all likely contribute to observed differences. IA has not been reported to occur spontaneously in patients that lack Dectin-1 expression (Ferwerda et al., 2009) or in pediatric patients with deficiency in the TLR adaptor protein MyD88 (von Bernuth et al., 2008), extending the concept of redundancy to Dectin-1 and MyD88 function.

The link between CARD9 and neutrophil conidial uptake was unexpected because CARD9 appears dispensable for BMM and BMDC zymosan uptake (Goodridge et al., 2009), a finding that we observed for AM conidial uptake in the lung. Following CLR ligation, CARD9 complexes with BCL10 and MALT1, a scaffold that is critical for NF-κB and MAPK activation (Gross et al., 2006; Hara et al., 2007; Hsu et al., 2007). In THP-1 monocytes, BCL10 silencing reduces phagocytosis of immunoglobulin-coated sheep RBCs by impairing phagocytic cup formation (Rueda et al., 2007). The release of soluble pattern recognition receptors, e.g., pentraxin-3, may enhance lung neutrophil conidial uptake (Moalli et al., 2010), and CARD9-dependent regulation of this activity may underlie the observed neutrophil conidial uptake defect.

Our study and other reports indicate that NADPH oxidase-deficient neutrophils have significant residual conidiacidal activity in vivo (Zarember et al., 2007). Neutrophil serine proteases are unlikely to contribute to this activity (Vethanayagam et al., 2011), consistent with the phenotype of patients with genetic defects in their activity (Pham, 2006). Whether calcineurin and NFAT-dependent activity contributes to conidiacidal activity remains to be elucidated (Greenblatt et al., 2010).

The development of IA represents a barometer of host innate immune function. The FLARE strain provides a means to interrogate the molecular and cellular elements that control phagocytic and cytotoxic responses in the lung. This approach will allow researchers to reconstruct the molecular events essential for conidial clearance in vivo. Improved understanding of these mechanisms may lead to prophylactic or therapeutic strategies for IA in at-risk patient populations. Harnessing fluorescence to trace microbial fate and to quantify leukocyte antimicrobial activity is likely to enhance studies of microbial pathogenesis and host immunity.

EXPERIMENTAL PROCEDURES

Chemical Reagents and Antibodies

Chemicals, cell culture reagents, and α-Dectin-2 monoclonal antibody (mAb) (clone D2.11E4) were from Sigma-Aldrich, GIBCO, and AbD Serotec, respectively.

Mice

Dectin-1$^{(-/-)}$ (Saijo et al., 2007), CARD9$^{(-/-)}$ (Hsu et al., 2007), and C57BL/6 (Jackson Laboratories) mice were housed in the Fred Hutchinson Cancer Research Center (FHCRC) Animal Health Resources Facility under specific pathogen-free conditions. BM chimeric mice were generated by reconstituting lethally irradiated (9.5 Gy) C57BL/6.SJL (CD45.1) with 2–5 × 10^6 Syk$^{(-/-)}$ (Mócsai et al., 2002), Dectin-1$^{(-/-)}$ (Saijo et al., 2007), CD18$^{(-/-)}$ (Scharffetter-Kochanek et al., 1998), or C57BL/6 BM cells and rested for 4–6 weeks prior to use. For some experiments, a 1:1 mixture of p47phox$^{(-/-)}$ (Jackson et al., 1995) and C57BL/6.SJL BM cells was infused into irradiated CD45.1$^+$ CD45.2$^+$ C57BL/6 recipients. All experiments were conducted with sex- and age-matched mice and performed with approval from the FHCRC Institutional Animal Care and Use Committee.

Generation of the FLARE Strain

Af293 conidia were transformed with pAN7-1 (Punt et al., 1987) and pPgpd-dsRed (Mikkelsen et al., 2003) using the method described by Sanchez and Aguirre (1996). Hygromycin-resistant transformants were screened by microscopy and flow cytometry for dsRed expression. One of eight transformants (Af293-dsRed) was selected for further use, based on bright fluorescence in all growth stages and equivalent radial growth on Sabouraud plates compared to the parental strain. To generate FLARE conidia, 5 × 10^8 Af293-dsRed

conidia were rotated in 0.5 mg/ml Biotin XX, SSE (B-6352; Invitrogen) in 1 ml 50 mM carbonate buffer (pH 8.3) for 2 hr at 4°C, washed in 0.1 M Tris-HCl (pH 8), labeled with 0.02 mg/ml AF633-streptavidin (S-21375; Invitrogen) in 1 ml PBS for 30 min at RT, and resuspended in PBS and 0.025% Tween 20 for experimental use.

Intratracheal Infection Model

For i.t. infections, mice were lightly anesthetized and immobilized in an upright position using rubber bands attached to a Plexiglas stand. A blunt 20G needle attached to a 1 ml syringe was advanced into the trachea to deliver the indicated number of conidia (typically 3×10^7) in a volume of 0.05 ml PBS, 0.025% Tween 20.

Analysis of Infected Mice

Infected mice were euthanized at indicated times, and the lungs were perfused, and homogenized in 2 ml of PBS, 0.025% Tween 20 for cfu analysis and ELISA assays. For histological studies, the lungs were inflated with 10% buffered formalin, fixed, and embedded in formalin to generate 4 μm sections stained with hematoxylin and eosin (H&E) or Gomori's ammoniacal silver (GAS) stain for microscopy using a TissueFAXS cytometer (TissueGnostics). Contiguous tissue sections were imaged using a Zeiss Plan Neofluar 403/0.75 objective and all fields merged into a single image using Tissue-FAXS Viewer, v. 3.0 software. Image analysis was performed using ImageJ software (v.1.46i). BAL neutrophils were sorted on a BD Aria sorter and analyzed by fluorescence microscopy on an Applied Precision DeltaVision microscope (403 Olympus objective, NA = 1.3) with identical settings for all image acquisition. DeltaVision software softWoRx 4.1.2 was used for image processing.

Single-cell lung suspensions were prepared for flow cytometric analysis and classified as described in Hohl et al. (2009). Tissue processing did not result in leukocyte uptake of exogenously added FLARE conidia. Lung digest and, if applicable, BAL cells were enumerated and stained with the following Abs: anti-Ly6C (clone AL-21), anti-Ly6G (clone 1A8), anti-CD11b (clone M1/70), anti-CD11c (clone HL3), anti-CD45.1 (clone A20), anti-CD45.2 (clone 104), and anti-Ly6B.2 (clone 7/4). PE- and APC-labeled Abs were omitted in FLARE experiments. AMs were identified as $SSC^{high}CD45^+CD11c^+$ BAL cells, and neutrophils were identified as $CD45^+CD11b^+Ly6C^{lo}Ly6G^+$ cells, or alternatively, as $CD45^+7/4^+Ly6G^+$ cells. Flow cytometry data were collected on a BD LSR II flow cytometer and analyzed with FlowJo, v.9.4.3 (TreeStar).

For imaging cytometry, BAL cells were lysed of RBCs, stained with CD45, 7/4, and Ly6G fluorescent antibodies, and fixed for 20 min in 1% paraformal-dehyde. Fixed cells were run on the ImageStreamX (Amnis, Seattle), and images were analyzed using IDEAS software.

In Vitro Conidial Kill Assay

For conidial kill assays, 2.5×10^5 FLARE conidia were incubated in 0.2 ml RP10 (Hohl et al., 2005) with 0–10 M H_2O_2 for 30 min at 37°C, washed, and analyzed by flow cytometry for dsRed and AF633 fluorescence. Duplicate samples were plated (at 1:1,000 dilution) to determine the cfu.

Neutrophil ROS Assay

BM cells were flushed from murine tibias and femurs, and neutrophils were harvested from the 62%–81% interface of a discontinuous (50%–55%–62%–81%) Percoll gradient. For ROS assays, cells were seeded in 0.1 ml HBSS (with Ca^{2+} and Mg^{2+}) in 96-well white opaque plates at a concentration of 10^6 cells/ml and stimulated with 2×10^5 UV-inactivated swollen conidia (swollen in RP10 for 6 hr at 37°C). ROS production was quantified using

the Diogenes reagent (CL 202; National Diagnostics) on a microplate luminometer (Model Centro LB960; Berthold) for 60 min according to the manufacturer's protocol. Resting conidia did not induce a measurable signal in the ROS assay. Phorbol myristate acetate (910 nM) stimulation was used as a nonspecific control for ROS production.

Statistical Analysis

All results are expressed as mean ± SEM derived from three independent experiments, unless stated otherwise. A Mann-Whitney U test (for two group comparisons) or a Kruskal-Wallis one-way ANOVA followed by Dunn's multiple comparison tests (for three group comparisons) were used for statistical analyses. Survival data were analyzed by log rank test. All statistical analyses were performed with GraphPad Prism software, v.5.0c. A p value <0.05 was considered significant and indicated with an asterisk.

For more details, please see the Extended Experimental Procedures.

Supplementary Material

Refer to Web version on PubMed Central for supplementary material.

Acknowledgments

This work was supported by National Institutes of Health grant R01 AI093809 (T.M.H.), National Institute of Allergy and Infectious Diseases grant R01AI079253 (B.H.S.), the Robert A. Sinskey Foundation (T.M.H.), Cancer Center Support Grants to FHCRC (P30 CA015704) and to the Roswell Park Cancer Institute (CA016056), and CREST and the Promotion of Basic Research Activities for Innovative Biosciences program (Y.I.). We thank Julie Randolph-Habecker and Sharon McLaughlin (Experimental Histopathology, FHCRC), Raymond Kong (Amnis, Seattle), and Lisbeth Mikkelsen (The Royal Veterinary and Agricultural University, Copenhagen, Denmark) for help with histopathology and imaging cytometry, and for plasmids pAN7-1 and pPgpd-dsRed, respectively. T.M.H. designed and supervised the study. A.J., K.B.M., D.K.K., L.Y.N., S.E.K., and T.M.H. performed experiments. X.L., C.A.L., Y.I., J.A.H., and B.H.S. contributed gene-deficient mice and provided scientific input. A.J. and T.M.H. analyzed data and wrote the manuscript. We thank Amariliz Rivera and Robert Cramer for critical reading of the manuscript.

REFERENCES

Balajee SA, Marr KA. Conidial viability assay for rapid susceptibility testing of *Aspergillus* species. J. Clin. Microbiol. 2002; 40:2741–2745. [PubMed: 12149322]

Bonnett CR, Cornish EJ, Harmsen AG, Burritt JB. Early neutrophil recruitment and aggregation in the murine lung inhibit germination of *Aspergillus fumigatus* Conidia. Infect. Immun. 2006; 74:6528–6539. [PubMed: 16920786]

Boyle KB, Gyori D, Sindrilaru A, Scharffetter-Kochanek K, Taylor PR, Mócsai A, Stephens LR, Hawkins PT. Class IA phosphoinositide 3-kinase β and δ regulate neutrophil oxidase activation in response to *Aspergillus fumigatus* hyphae. J. Immunol. 2011; 186:2978–2989. [PubMed: 21257963]

Brothers KM, Newman ZR, Wheeler RT. Live imaging of disseminated candidiasis in zebrafish reveals role of phagocyte oxidase in limiting filamentous growth. Eukaryot. Cell. 2011; 10:932–944. [PubMed: 21551247]

Brown GD. Innate antifungal immunity: the key role of phagocytes. Annu. Rev. Immunol. 2011; 29:1–21. [PubMed: 20936972]

Carvalho A, Giovannini G, De Luca A, D'Angelo C, Casagrande A, Iannitti RG, Ricci G, Cunha C, Romani L. Dectin-1 isoforms contribute to distinct Th1/Th17 cell activation in mucosal candidiasis. Cell. Mol. Immunol. 2012; 9:276–286. [PubMed: 22543832]

Chai LY, de Boer MG, van der Velden WJ, Plantinga TS, van Spriel AB, Jacobs C, Halkes CJ, Vonk AG, Blijlevens NM, van Dissel JT, et al. The Y238X stop codon polymorphism in the human β-glucan receptor dectin-1 and susceptibility to invasive aspergillosis. J. Infect. Dis. 2011; 203:736–743. [PubMed: 21242599]

Coombes JL, Robey EA. Dynamic imaging of host-pathogen interactions in vivo. Nat. Rev. Immunol. 2010; 10:353–364. [PubMed: 20395980]

Cunha C, Di Ianni M, Bozza S, Giovannini G, Zagarella S, Zelante T, D'Angelo C, Pierini A, Pitzurra L, Falzetti F, et al. Dectin-1 Y238X polymorphism associates with susceptibility to invasive aspergillosis in hematopoietic transplantation through impairment of both recipient- and donor-dependent mechanisms of antifungal immunity. Blood. 2010; 116:5394–5402. [PubMed: 20807886]

Ferwerda B, Ferwerda G, Plantinga TS, Willment JA, van Spriel AB, Venselaar H, Elbers CC, Johnson MD, Cambi A, Huysamen C, et al. Human dectin-1 deficiency and mucocutaneous fungal infections. N. Engl. J. Med. 2009; 361:1760–1767. [PubMed: 19864674]

Gerson SL, Talbot GH, Hurwitz S, Strom BL, Lusk EJ, Cassileth PA. Prolonged granulocytopenia: the major risk factor for invasive pulmonary aspergillosis in patients with acute leukemia. Ann. Intern. Med. 1984; 100:345–351. [PubMed: 6696356]

Gersuk GM, Underhill DM, Zhu L, Marr KA. Dectin-1 and TLRs permit macrophages to distinguish between different *Aspergillus fumigatus* cellular states. J. Immunol. 2006; 176:3717–3724. [PubMed: 16517740]

Glocker EO, Hennigs A, Nabavi M, Schäffer AA, Woellner C, Salzer U, Pfeifer D, Veelken H, Warnatz K, Tahami F, et al. A homozygous CARD9 mutation in a family with susceptibility to fungal infections. N. Engl. J. Med. 2009; 361:1727–1735. [PubMed: 19864672]

Goodridge HS, Shimada T, Wolf AJ, Hsu YM, Becker CA, Lin X, Underhill DM. Differential use of CARD9 by dectin-1 in macrophages and dendritic cells. J. Immunol. 2009; 182:1146–1154. [PubMed: 19124758]

Greenblatt MB, Aliprantis A, Hu B, Glimcher LH. Calcineurin regulates innate antifungal immunity in neutrophils. J. Exp. Med. 2010; 207:923–931. [PubMed: 20421389]

Gringhuis SI, den Dunnen J, Litjens M, van der Vlist M, Wevers B, Bruijns SC, Geijtenbeek TB. Dectin-1 directs T helper cell differentiation by controlling noncanonical NF-kappaB activation through Raf-1 and Syk. Nat. Immunol. 2009; 10:203–213. [PubMed: 19122653]

Gross O, Gewies A, Finger K, Schäfer M, Sparwasser T, Peschel C, Förster I, Ruland J. Card9 controls a non-TLR signalling pathway for innate anti-fungal immunity. Nature. 2006; 442:651–656. [PubMed: 16862125]

Hara H, Ishihara C, Takeuchi A, Imanishi T, Xue L, Morris SW, Inui M, Takai T, Shibuya A, Saijo S, et al. The adaptor protein CARD9 is essential for the activation of myeloid cells through ITAM-associated and Toll-like receptors. Nat. Immunol. 2007; 8:619–629. [PubMed: 17486093]

Herre J, Marshall AS, Caron E, Edwards AD, Williams DL, Schweighoffer E, Tybulewicz V, Reis e Sousa C, Gordon S, Brown GD. Dectin-1 uses novel mechanisms for yeast phagocytosis in macrophages. Blood. 2004; 104:4038–4045. [PubMed: 15304394]

Hohl TM, Van Epps HL, Rivera A, Morgan LA, Chen PL, Feldmesser M, Pamer EG. *Aspergillus fumigatus* triggers inflammatory responses by stage-specific beta-glucan display. PLoS Pathog. 2005; 1:e30. [PubMed: 16304610]

Hohl TM, Rivera A, Lipuma L, Gallegos A, Shi C, Mack M, Pamer EG. Inflammatory monocytes facilitate adaptive CD4 T cell responses during respiratory fungal infection. Cell Host Microbe. 2009; 6:470–481. [PubMed: 19917501]

Hsu YM, Zhang Y, You Y, Wang D, Li H, Duramad O, Qin XF, Dong C, Lin X. The adaptor protein CARD9 is required for innate immune responses to intracellular pathogens. Nat. Immunol. 2007; 8:198–205. [PubMed: 17187069]

Ibrahim-Granet O, Philippe B, Boleti H, Boisvieux-Ulrich E, Grenet D, Stern M, Latgé JP. Phagocytosis and intracellular fate of *Aspergillus fumigatus* conidia in alveolar macrophages. Infect. Immun. 2003; 71:891–903. [PubMed: 12540571]

Jackson SH, Gallin JI, Holland SM. The p47phox mouse knock-out model of chronic granulomatous disease. J. Exp. Med. 1995; 182:751–758. [PubMed: 7650482]

Kauffman CA, Pappas PG, Patterson TF. Fungal infections associated with contaminated methylprednisolone injections—preliminary report. N. Engl. J. Med. Published online October. 2012; 19 2012. http://dx.doi.org/10.1056/NEJMra1212617.

Leal SM Jr. Cowden S, Hsia YC, Ghannoum MA, Momany M, Pearlman E. Distinct roles for Dectin-1 and TLR4 in the pathogenesis of *Aspergillus fumigatus* keratitis. PLoS Pathog. 2010; 6:e1000976. [PubMed: 20617171]

Leal SM Jr. Vareechon C, Cowden S, Cobb BA, Latgé JP, Momany M, Pearlman E. Fungal antioxidant pathways promote survival against neutrophils during infection. J. Clin. Invest. 2012; 122:2482–2498. [PubMed: 22706306]

LeibundGut-Landmann S, Gross O, Robinson MJ, Osorio F, Slack EC, Tsoni SV, Schweighoffer E, Tybulewicz V, Brown GD, Ruland J, Reis e Sousa C. Syk- and CARD9-dependent coupling of innate immunity to the induction of T helper cells that produce interleukin 17. Nat. Immunol. 2007; 8:630–638. [PubMed: 17450144]

LeibundGut-Landmann S, Wüthrich M, Hohl TM. Immunity to fungi. Curr. Opin. Immunol. 2012; 24:449–458. [PubMed: 22613091]

Li X, Utomo A, Cullere X, Choi MM, Milner DA Jr. Venkatesh D, Yun SH, Mayadas TN. The β-glucan receptor Dectin-1 activates the integrin Mac-1 in neutrophils via Vav protein signaling to promote *Candida albicans* clearance. Cell Host Microbe. 2011; 10:603–615. [PubMed: 22177564]

Looney MR, Thornton EE, Sen D, Lamm WJ, Glenny RW, Krummel MF. Stabilized imaging of immune surveillance in the mouse lung. Nat. Methods. 2011; 8:91–96. [PubMed: 21151136]

Maselli A, Laevsky G, Knecht DA. Kinetics of binding, uptake and degradation of live fluorescent (DsRed) bacteria by *Dictyostelium discoideum*. Microbiology. 2002; 148:413–420. [PubMed: 11832505]

Mehrad B, Strieter RM, Moore TA, Tsai WC, Lira SA, Standiford TJ. CXC chemokine receptor-2 ligands are necessary components of neutrophil-mediated host defense in invasive pulmonary aspergillosis. J. Immunol. 1999; 163:6086–6094. [PubMed: 10570298]

Mertens JA, Skory CD, Ibrahim AS. Plasmids for expression of heterologous proteins in Rhizopus oryzae. Arch. Microbiol. 2006; 186:41–50. [PubMed: 16804680]

Miesenböck G, De Angelis DA, Rothman JE. Visualizing secretion and synaptic transmission with pH-sensitive green fluorescent proteins. Nature. 1998; 394:192–195. [PubMed: 9671304]

Mikkelsen L, Sarrocco S, Lübeck M, Jensen DF. Expression of the red fluorescent protein DsRed-Express in filamentous ascomycete fungi. FEMS Microbiol. Lett. 2003; 223:135–139. [PubMed: 12799012]

Mircescu MM, Lipuma L, van Rooijen N, Pamer EG, Hohl TM. Essential role for neutrophils but not alveolar macrophages at early time points following *Aspergillus fumigatus* infection. J. Infect. Dis. 2009; 200:647–656. [PubMed: 19591573]

Moalli F, Doni A, Deban L, Zelante T, Zagarella S, Bottazzi B, Romani L, Mantovani A, Garlanda C. Role of complement and Fcgamma receptors in the protective activity of the long pentraxin PTX3 against *Aspergillus fumigatus*. Blood. 2010; 116:5170–5180. [PubMed: 20829368]

Mócsai A, Zhou M, Meng F, Tybulewicz VL, Lowell CA. Syk is required for integrin signaling in neutrophils. Immunity. 2002; 16:547–558. [PubMed: 11970878]

Mócsai A, Ruland J, Tybulewicz VL. The SYK tyrosine kinase: a crucial player in diverse biological functions. Nat. Rev. Immunol. 2010; 10:387–402. [PubMed: 20467426]

Park SJ, Mehrad B. Innate immunity to *Aspergillus* species. Clin. Microbiol. Rev. 2009; 22:535–551. [PubMed: 19822887]

Pettit AC, Kropski JA, Castilho JL, Schmitz JE, Rauch CA, Mobley BC, Wang XJ, Spires SS, Pugh ME. The index case for the fungal meningitis outbreak in the United States. N. Engl. J. Med. 2012 Published online October 19, 2012. http://dx.doi.org/10.1056/NEJMoa1212292.

Pham CT. Neutrophil serine proteases: specific regulators of inflammation. Nat. Rev. Immunol. 2006; 6:541–550. [PubMed: 16799473]

Philippe B, Ibrahim-Granet O, Prévost MC, Gougerot-Pocidalo MA, Sanchez Perez M, Van der Meeren A, Latgé JP. Killing of *Aspergillus fumigatus* by alveolar macrophages is mediated by reactive oxidant intermediates. Infect. Immun. 2003; 71:3034–3042. [PubMed: 12761080]

Punt PJ, Oliver RP, Dingemanse MA, Pouwels PH, van den Hondel CA. Transformation of *Aspergillus* based on the hygromycin B resistance marker from Escherichia coli. Gene. 1987; 56:117–124. [PubMed: 2824287]

Rivera A, Hohl TM, Collins N, Leiner I, Gallegos A, Saijo S, Coward JW, Iwakura Y, Pamer EG. Dectin-1 diversifies *Aspergillus fumigatus*-specific T cell responses by inhibiting T helper type 1 CD4 T cell differentiation. J. Exp. Med. 2011; 208:369–381. [PubMed: 21242294]

Rodriguez TE, Falkowski NR, Harkema JR, Huffnagle GB. Role of neutrophils in preventing and resolving acute fungal sinusitis. Infect. Immun. 2007; 75:5663–5668. [PubMed: 17875637]

Rueda D, Gaide O, Ho L, Lewkowicz E, Niedergang F, Hailfinger S, Rebeaud F, Guzzardi M, Conne B, Thelen M, et al. Bcl10 controls TCR- and FcgammaR-induced actin polymerization. J. Immunol. 2007; 178:4373–4384. [PubMed: 17371994]

Saijo S, Fujikado N, Furuta T, Chung SH, Kotaki H, Seki K, Sudo K, Akira S, Adachi Y, Ohno N, et al. Dectin-1 is required for host defense against *Pneumocystis carinii* but not against Candida albicans. Nat. Immunol. 2007; 8:39–46. [PubMed: 17159982]

Sanchez O, Aguirre J. Efficient transformation of *Aspergillus nidulans* by electroporation of germinated conidia. Fungal Genet. Newsl. 1996; 43:48–51.

Scharffetter-Kochanek K, Lu H, Norman K, van Nood N, Munoz F, Grabbe S, McArthur M, Lorenzo I, Kaplan S, Ley K, et al. Spontaneous skin ulceration and defective T cell function in CD18 null mice. J. Exp. Med. 1998; 188:119–131. [PubMed: 9653089]

Steele C, Rapaka RR, Metz A, Pop SM, Williams DL, Gordon S, Kolls JK, Brown GD. The beta-glucan receptor dectin-1 recognizes specific morphologies of *Aspergillus fumigatus*. PLoS Pathog. 2005; 1:e42. [PubMed: 16344862]

Tobin DM, May RC, Wheeler RT. Zebrafish: a see-through host and a fluorescent toolbox to probe host-pathogen interaction. PLoS Pathog. 2012; 8:e1002349. [PubMed: 22241986]

Underhill DM, Rossnagle E, Lowell CA, Simmons RM. Dectin-1 activates Syk tyrosine kinase in a dynamic subset of macrophages for reactive oxygen production. Blood. 2005; 106:2543–2550. [PubMed: 15956283]

Van Ziffle JA, Lowell CA. Neutrophil-specific deletion of Syk kinase results in reduced host defense to bacterial infection. Blood. 2009; 114:4871–4882. [PubMed: 19797524]

Vethanayagam RR, Almyroudis NG, Grimm MJ, Lewandowski DC, Pham CT, Blackwell TS, Petraitiene R, Petraitis V, Walsh TJ, Urban CF, Segal BH. Role of NADPH oxidase versus neutrophil proteases in antimicrobial host defense. PLoS One. 2011; 6:e28149. [PubMed: 22163282]

von Bernuth H, Picard C, Jin Z, Pankla R, Xiao H, Ku CL, Chrabieh M, Mustapha IB, Ghandil P, Camcioglu Y, et al. Pyogenic bacterial infections in humans with MyD88 deficiency. Science. 2008; 321:691–696. [PubMed: 18669862]

Wasylnka JA, Moore MM. Uptake of *Aspergillus fumigatus* Conidia by phagocytic and nonphagocytic cells in vitro: quantitation using strains expressing green fluorescent protein. Infect. Immun. 2002; 70:3156–3163. [PubMed: 12011010]

Werner JL, Metz AE, Horn D, Schoeb TR, Hewitt MM, Schwiebert LM, Faro-Trindade I, Brown GD, Steele C. Requisite role for the dectin-1 beta-glucan receptor in pulmonary defense against *Aspergillus fumigatus*. J. Immunol. 2009; 182:4938–4946. [PubMed: 19342673]

Werner JL, Gessner MA, Lilly LM, Nelson MP, Metz AE, Horn D, Dunaway CW, Deshane J, Chaplin DD, Weaver CT, et al. Neutrophils produce interleukin 17A (IL-17A) in a dectin-1- and IL-23-dependent manner during invasive fungal infection. Infect. Immun. 2011; 79:3966–3977. [PubMed: 21807912]

Wu W, Hsu YM, Bi L, Songyang Z, Lin X. CARD9 facilitates microbe-elicited production of reactive oxygen species by regulating the LyGDI-Rac1 complex. Nat. Immunol. 2009; 10:1208–1214. [PubMed: 19767757]

Zarember KA, Sugui JA, Chang YC, Kwon-Chung KJ, Gallin JI. Human polymorphonuclear leukocytes inhibit *Aspergillus fumigatus* conidial growth by lactoferrin-mediated iron depletion. J. Immunol. 2007; 178:6367–6373. [PubMed: 17475866]

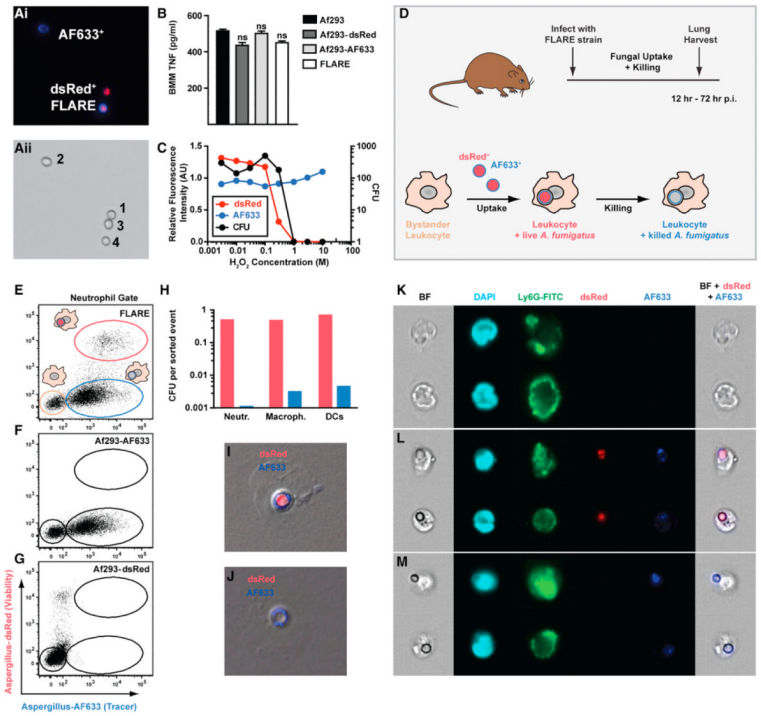

Figure 1. FLARE Conidia Report Conidial Uptake and Killing In Vitro and In Vivo

(Ai) Fluorescence and (Aii) transmitted light micrographs of (1) Af293, (2) Af293-AF633, (3) Af293-dsRed, and (4) Af293-dsRed-AF633 (FLARE) conidia.

(B) The graph shows the average (±SEM) BMM TNF release following coincubation with Af293 (black bar), Af293-dsRed (dark-gray bar), Af293-AF633 (light-gray bar), and FLARE (white bar) conidia at a multiplicity of infection (moi) of 5 (four replicates per strain). ns, not significant.

(C) The graph shows dsRed (red) and AF633 (blue) fluorescence and cfu (black circles) from FLARE conidia exposed to the indicated H_2O_2 concentration. Mean fluorescence intensity is indicated relative to FLARE conidia not treated with H_2O_2.

(D) Scheme of fluorescence changes associated with leukocyte conidial uptake and killing. Bystander leukocytes acquire dsRed and AF633 fluorescence after engulfing FLARE conidia. Loss of dsRed and retention of AF633 fluorescence coincide with conidial killing.

(E–G) The plots show lung neutrophils from (E) FLARE-infected, (F) Af293-AF633-infected, or (G) Af293-dsRed-infected mice (inoculum: 3×10^7 conidia) analyzed for dsRed and AF633 fluorescence 36 hr p.i.

(H) The graph shows fungal cfu (per sorted event) recovered from sorted $dsRed^+AF633^+$ (red bars) or $dsRed^-AF633^+$ (blue bars) lung neutrophils (Neutr.), macrophages (Macroph.), and $CD11b^+$ DCs 36 hr p.i.

(I–M) Fluorescence microscopy (I and J) and imaging cytometry (K–M) of BAL neutrophils from FLARE-infected mice. The micrographs depict sorted $dsRed^+AF633^+$ (I and L) and $dsRed^-AF633^+$ (J and M) and $dsRed^-AF633^-$ neutrophils (K). The columns in (K–M) show bright-field (BF), DAPI, Ly6G, dsRed, and AF633 channels, with composite micrographs (BF, dsRed, and AF633) at the far right.

Data are representative from 1 (B), 2 (C), >20 (E–G), or 3 (H–J) experiments.

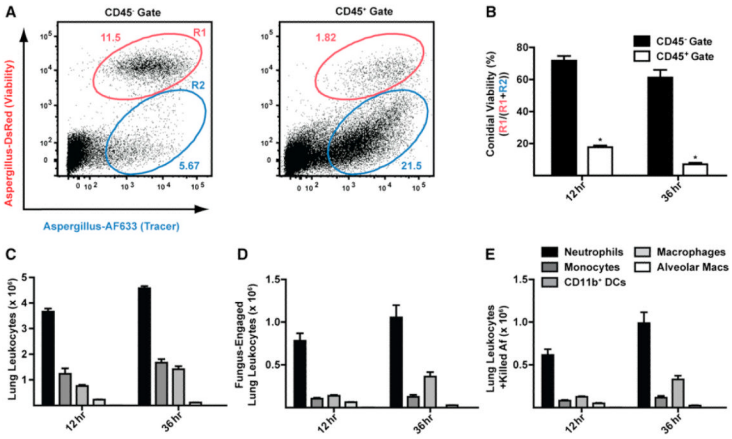

Figure 2. FLARE Conidia Undergo Leukocyte-Dependent Killing in the Lung

C57BL/6 mice were infected with 3×10^7 FLARE conidia, and single-cell lung suspensions were stained for CD45 and analyzed for dsRed and AF633 fluorescence.

(A) Representative plots show live (R1; red gate) and killed conidia (R2; blue gate) in the $CD45^-$ or in the $CD45^+$ gate at 36 hr p.i.

(B) The bar graphs show the average (±SEM) conidial viability in the $CD45^-$ and $CD45^+$ gates (n = 5 per group). *$p < 0.05$ (Mann-Whitney U test).

(C–E) The bar graphs show the average number (±SEM) of (C) leukocytes, (D) fungus-engaged leukocytes, and (E) leukocytes containing killed conidia in FLARE-infected lungs 36 hr p.i. Neutrophils are indicated in black bars, monocytes in dark-gray bars, $CD11b^+$ DCs in gray bars, lung macrophages in light-gray bars, and AMs in white bars.

The data in (A–E) are from a representative experiment from more than ten experiments performed with five mice per time point.

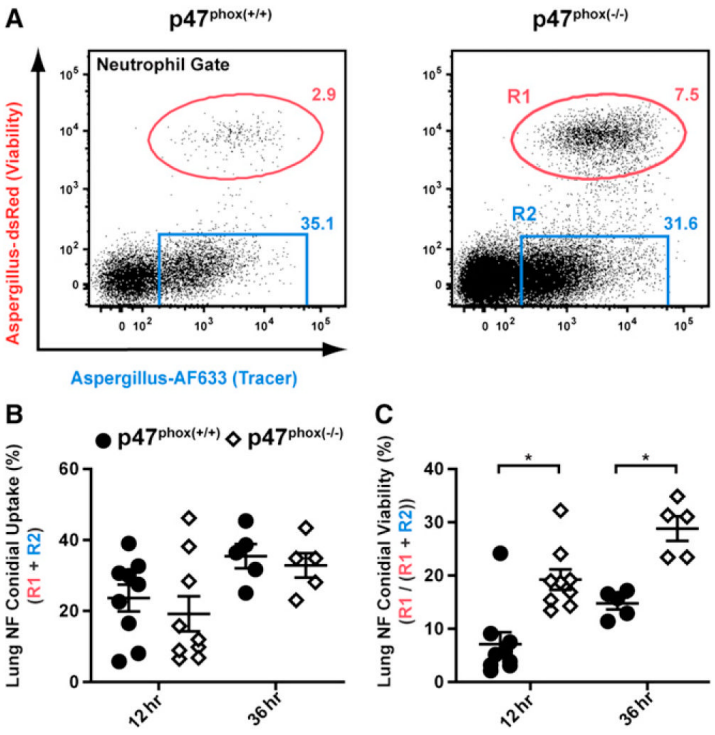

Figure 3. NADPH Oxidase Mediates Neutrophil-Dependent Conidial Killing in the Lung

BM chimeric mice (1:1 mix of $CD45.1^+p47^{phox(+/+)}$ and $CD45.2^+p47^{phox(-/-)}$ BM cells → irradiated $CD45.1^+CD45.2^+$ recipients) were infected with 3×10^7 FLARE conidia.

(A) Representative plots of $p47^{phox(+/+)}$ and $p47^{phox(-/-)}$ neutrophils analyzed for dsRed and AF633 fluorescence show the frequencies of neutrophils that contain live (red gate) or killed (blue gate) conidia 36 hr p.i.

(B and C) Scatterplots from one (36 hr p.i.) or two (12 hr p.i.) experiments show the average frequency (±SEM) of (B) lung neutrophil conidial uptake (R1 + R2) and (C) lung neutrophil conidial viability (R1/(R1 + R2)) by $p47^{phox(+/+)}$ (circles) or $p47^{phox(-/-)}$ (diamonds) neutrophils. *$p < 0.05$ (paired t test).

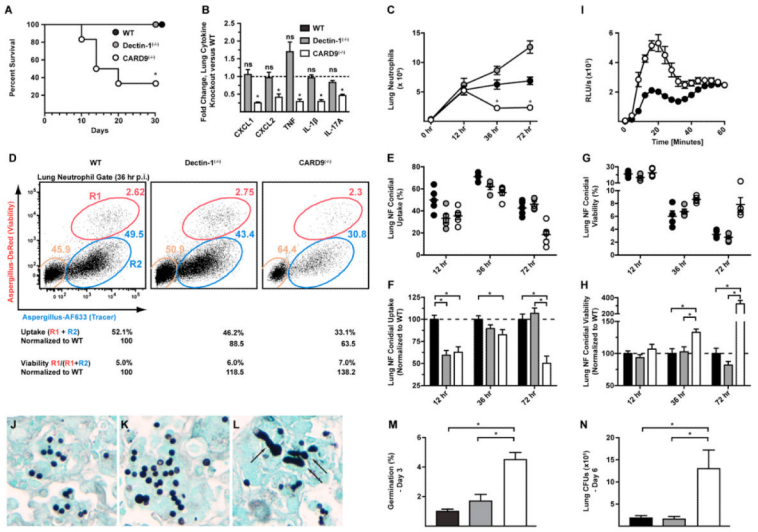

Figure 4. CARD9 and Neutrophil Function during Respiratory Fungal Infection

WT (black circles or bars), Dectin-1$^{(-/-)}$ (gray circles or bars), and CARD9$^{(-/-)}$ (white circles or bars) mice were infected via the i.t. route with 8 × 10^7 Af293 (A and J–M) or 3 × 10^7 FLARE conidia (B–H and N).

(A) Kaplan-Meier survival of WT (n = 8), Dectin-1$^{(-/-)}$ (n = 6), and CARD9$^{(-/-)}$ (n = 6) mice from a representative experiment.

(B) Lung cytokines 36 hr p.i. expressed as the fold change (±SEM) in the (−/−) response compared to the (+/+) response pooled from four experiments.

(C) Neutrophil recruitment (±SEM) from 8–14 mice, pooled from two to three experiments per time point.

(D) Flow cytometry plots of lung neutrophils from FLARE-infected WT, Dectin-1$^{(-/-)}$, and CARD9$^{(-/-)}$ mice. The tan gates indicate bystander neutrophils, and the red (R1) and blue (R2) gates indicate neutrophils that contain live or killed conidia, respectively.

(E and G) The plots show neutrophil conidial uptake (R1 + R2) and conidial viability ((R1/(R1 + R2)) (±SEM) in WT, Dectin-1$^{(-/-)}$, and CARD9$^{(-/-)}$ mice at 12, 36, and 72 hr p.i. from a representative experiment.

(F and H) The plots show the mean (±SEM) neutrophil conidial uptake and viability using normalized data pooled from four (12 hr), three (36 hr), and two (72 hr) experiments, each with four to five mice per group and time point.

(I) ROS generation by BM neutrophils isolated from WT and CARD9$^{(-/-)}$ mice and stimulated with swollen conidia. Data are expressed as RLU/s (×10^3) (mean ± SEM).

(J–L) Representative images of silver-stained lung sections (40×) from WT (J), Dectin-1$^{(-/-)}$ (K), and CARD9$^{(-/-)}$ (L) mice at 3 days p.i.

(M) The graph shows the average frequency (±SEM) of germlings in murine lungs 3 days p.i. indicated by arrows in (L). A total of 5,000–7,000 fungal elements were enumerated using sections from two mice per genotype.

(N) The graph shows the average (±SEM) lung fungal burden 6 days p.i. The data are pooled from two experiments, each with four to five mice per group.

*p < 0.05 (one-way ANOVA). See also Figures S1, S2, S3, and S4.

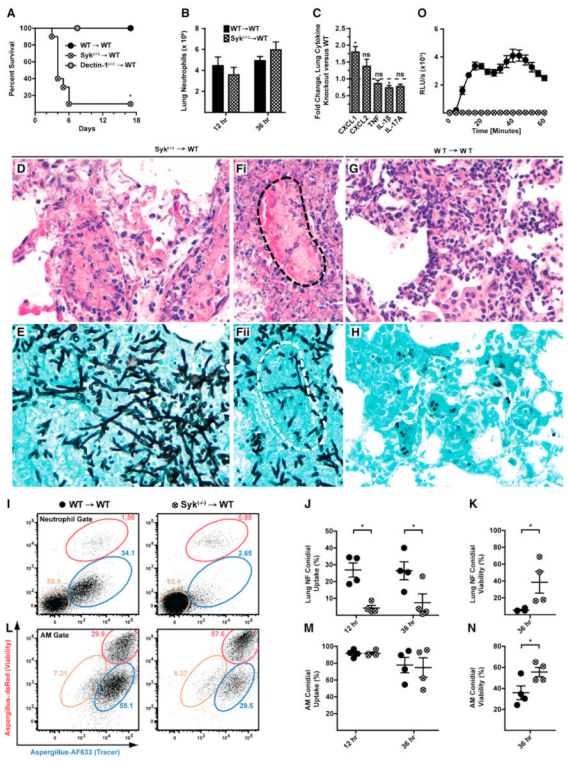

Figure 5. Syk and Neutrophil Function during Respiratory Fungal Infection

(A–N) Syk$^{(-/-)}$ → WT (hatched circles or bars) and WT → WT (black circles or bars) mice were infected with (A and D–H) Af293 or (B, C, and I–N) FLARE conidia and euthanized at the indicated times p.i.

(A) Kaplan-Meier survival plot of Syk$^{(-/-)}$ → WT (n = 10), Dectin-1$^{(-/-)}$→ WT (n = 5), and WT → WT (n = 10) mice challenged with 2–5 × 10^7 conidia. The data are pooled from two experiments.

(B and C) The bar graphs show the average (±SEM) (B) lung neutrophil recruitment and (C) lung cytokines at 36 hr p.i. Lung cytokine data are expressed as the fold change in the (−/−) response compared to the (+/+) response pooled from two experiments, each with three to four mice per group.

(D–H) Representative micrographs of H&E (D, Fi, and G) and silver-stained (E, Fii, and H) lung sections from Syk$^{(-/-)}$ → WT (D, E, Fi, and Fii) and WT → WT (G and H) mice (40×). The dotted lines (black in Fi and white in Fii) show a blood vessel infiltrated by hyphae.

(I and L) Representative flow cytometry plots are gated on WT (left column) or Syk$^{(-/-)}$ (right column) (I) lung neutrophils or (L) AMs and analyzed as described in Figure 4.

(J, K, M, and N) The scatterplots indicate the mean (±SEM) (J and M) conidial uptake and (K and N) conidial viability in Syk$^{(-/-)}$ and WT, (J and K) neutrophils, and (M and N) AMs. Data from one of two experiments are shown.

(O) ROS generation by BM neutrophils isolated from WT → WT and Syk$^{(-/-)}$ → WT mice and stimulated with swollen conidia. Data are expressed as RLU/s (×10^3) (mean ± SEM).

*$p < 0.05$ (Mann-Whitney U test). See also Figure S5.